Nano-Structures & Nano-Objects 2 (2015) 11–18

Contents lists available at ScienceDirect

Nano-Structures & Nano-Objects

journal homepage: www.elsevier.com/locate/nanoso

Iridium@graphene composite nanomaterials synthesized in ionic liquid as re-usable catalysts for solvent-free hydrogenation of benzene and cyclohexene

Raquel Marcos Esteban [a], Kai Schütte [a], Philipp Brandt [a], Dorothea Marquardt [a], Hajo Meyer [a], Fabian Beckert [b], Rolf Mülhaupt [b,c], Hartmuth Kölling [d], Christoph Janiak [a,*]

[a] Institut für Anorganische Chemie und Strukturchemie, Heinrich Heine Universität Düsseldorf, 40204 Düsseldorf, Germany

[b] Freiburger Material Forschungszentrum (FMF) and Institut für Makromolekulare Chemie, Universität Freiburg, Stefan-Meier-Str. 21-31, 79104 Freiburg, Germany

[c] FRIAS, Freiburg Institute for Advanced Studies, Albertstr. 19, 79104 Freiburg, Germany

[d] Herotron E-Beam Service GmbH, Guardianstrasse 6-10, 06766 Bitterfeld-Wolfen, Germany

HIGHLIGHTS

- Easy iridium nanoparticle synthesis and deposition on graphene in ionic liquids (ILs).
- Rapid synthesis by microwave or electron-beam irradiation of Ir-carbonyl in ILs.
- Ir-nanoparticles on graphene as stable, re-usable hydrogenation catalyst.
- Synthesis and catalytic use of stable 2–5 nm Ir-nanoparticles on graphene.
- Hydrogenation catalysis under solvent-free conditions with easy catalyst recycling.

GRAPHICAL ABSTRACT

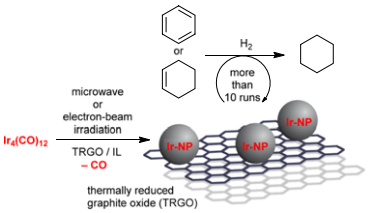

Iridium nanoparticles (Ir-NPs) can easily and quickly be prepared by microwave or electron-beam irradiation from the metal carbonyl in ionic liquids (IL), supported on graphene and show high and stable catalytic activities over several runs in benzene or cyclohexene hydrogenation reactions under organic-solvent-free and mild conditions.

ARTICLE INFO

Article history:
Received 16 July 2015
Accepted 20 July 2015

Keywords:
Iridium nanoparticles
Graphene
Thermally reduced graphite oxide, TRGO
Benzene hydrogenation
Catalysis

ABSTRACT

Synthesis of stable hybrid iridium@graphene nanomaterials in the ionic liquid (IL) 1-butyl-3-methylimidazolium tetrafluoroborate ([BMIm][BF_4] through microwave irradiation (MWI) or electron-beam (e-beam) irradiation (IBA Rhodotron accelerator) induced decomposition of $Ir_4(CO)_{12}$ in the presence of graphene provides an easy method for the generation of small iridium nanoparticles with size distributions of 1.0 ± 0.4 and 2.7 ± 0.7 nm by MWI reactions with 90 and 60 min decomposition time, respectively, and of 3.6 ± 1.0 nm for e-beam irradiation synthesis. Graphene was derived by thermal reduction of graphite oxide (TRGO). Powder X-ray diffraction (PXRD), transmission electron microscopy (TEM) and energy-dispersive X-ray spectrometry (EDX) showed the formation of Ir nanoparticles which are evenly distributed on the TRGO sheets. Ir@TRGO proved to be a highly active (~10 000 mol cyclohexane x(mol Ir)$^{-1}$x h^{-1} for benzene hydrogenation) and selective heterogeneous catalyst for the industrially relevant hydrogenation of benzene or cyclohexene to cyclohexane under mild conditions (100 °C, 10 bar H_2) with quantitative conversion. The catalyst could be re-used over 10 consecutive hydrogenation reactions with similar activities. A brief correlation between activity and particle size points to an optimal diameter or surface regime for the catalytic activity with iridium particles of 3.6 ± 1.0 nm on TRGO giving here the highest activity in benzene hydrogenation.

© 2015 Elsevier B.V.
This is an open access article under the CC BY-NC-ND license (http://creativecommons.org/licenses/by-nc-nd/4.0/).

* Corresponding author. Tel.: +49 211 81 12286; fax: +49 211 81 12287.
E-mail address: janiak@uni-duesseldorf.de (C. Janiak).

http://dx.doi.org/10.1016/j.nanoso.2015.07.001
2352-507X/© 2015 Elsevier B.V. This is an open access article under the CC BY-NC-ND license (http://creativecommons.org/licenses/by-nc-nd/4.0/).

1. Introduction

New methods and techniques for the synthesis of metal nanoparticles (M-NPs) have increased in the last five years due to their applications in fields of medicine [1], industry [2] or science [3]. The high surface area and thereby large number of active centers make the metal nanoparticle dispersions very attractive catalysts [4,5].

Typical syntheses of metal nanoparticles in aqueous or organic solutions need the presence of capping ligands, surfactants or polymer coating as stabilizer around the metal nanoparticle to prevent their aggregation and agglomeration in Ostwald ripening processes [6–8]. In recent years ionic liquids were developed into an alternative to traditional solvents [9,10]. The electrostatic and steric properties of ionic liquids (ILs) as molten salts do not require additional stabilizing ligands around the metal nanoparticles [11–13]. The possibility to prepare ligand-free, sometimes called "naked" metal nanoparticles (M-NPs) is advantageous for catalytic applications [13]. The high ionic charge, polarity and dielectric constant of ILs gives them a very high absorption efficiency for microwave irradiation (MWI) and allows for rapid microwave heating during precursor decomposition for nanoparticle synthesis [14–20]. Nanoparticle synthesis in ILs can be achieved from metal salts with [21–24] or without reducing H_2 gas [25–27], organometallic π-complexes [28–33] and metal carbonyls [17,18, 34–39] through thermal or photochemical [40,41] decomposition or electroreduction/ electrodeposition [11,42,43].

M-NP/IL dispersions as catalytic systems can be also re-used and recycled for many times, showing no loss of efficient and catalytic activity [18,44,45]. Biphasic (liquid–liquid) homogeneous-catalytic systems [6] often exhibit leaching of metal ions to the products, making their separation and purification process economically and environmentally more complicated. To avoid these problems, the research and development of new quasi-homogeneous nanoparticle catalyst systems is growing in the last few years [46,47].

Carbon-based materials like carbon nanotubes (CNTs) [48–50] are long known substrates for the deposition of metal nanoparticles. Nowadays a novel attractive material of the carbon family is thermally reduced graphite oxide (TRGO) also commonly named "*graphene*" [51]. Its tunable properties introduce this material as a novel support material for the deposition of metal nanoparticles such as Au- [52], Cu- [53], Pt- [54], Rh- or Ru-NPs [36,55] among others.

M-NPs synthesized using electron-beam (e-beam) irradiation are already reported in the literature. Uranium dioxide (UO_2) nanoparticles were obtained by electron beam irradiation of 7 MeV [56]. Cadmium selenide nanoparticles (CdSe) could also be synthesized by electron beam irradiation of aqueous butanol solutions with equimolar amounts of $Cd(NH_3)_4SO_4$ and Na_2SeSO_3 [57,58]. Also, gold/iron oxide composite were reported using a high-energy electron-beam irradiation [59].

Here we report the synthesis of iridium nanoparticles in ionic liquids with small size and narrow size distribution and their in situ deposition on thermally derived graphite oxide (Ir@TRGO). The energy input for metal-precursor decomposition can subtly influence the decomposition kinetics, nucleation and growth processes of nanocrystals. Thus, two different methods (MWI and e-beam irradiation) are also compared here for their possible influence in the synthesis of metal nanoparticles. The hybrid materials were tested for the industrially relevant catalytic hydrogenation of benzene and cyclohexene to cyclohexane [60,61].

2. Results and discussion

2.1. Synthesis and characterization of supported iridium nanoparticles

Iridium nanoparticles were obtained through thermal decomposition of $Ir_4(CO)_{12}$ by means of microwave irradiation (MWI) or e-beam irradiation (IBA Rhodotron accelerator) in 1-butyl-3-methyl-imidazolium tetrafluoroborate ([BMIm][BF_4]). The concomitant decomposition of tetrairidium dodecacarbonyl, $Ir_4(CO)_{12}$ and exfoliation of TRGO in [BMIm][BF_4] were achieved using the energy input by microwave (200 W, 250 °C, 90 min (**1a**) or 3 × 20 min (**1b**)) or e-beam irradiation (10 MeV, 3 × 1 s (**2**)) (Scheme 1).

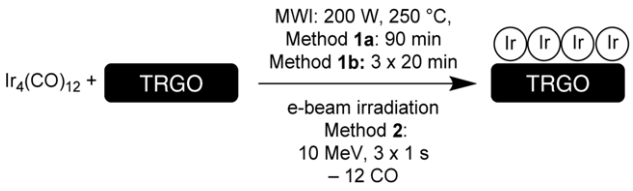

Scheme 1. Schematic synthesis of iridium@graphene nanomaterials in [BMIm][BF_4].

Powder X-ray diffractograms (PXRD) of the Ir@TRGO composites show the characteristic reflections at 2ϑ values of 40.7°, 46.8°, 68.6° and 83.3° corresponding to the (111), (002), (022) and (113) reflection of iridium metal (Fig. 1 and Fig. S2). Yet, a low intensity, high background and broad peaks indicate that the Ir-NPs are small and/or of low crystallinity. A particle-size determination by the Scherrer equation gave a diameter of 1.2 nm for the method **1a** and of 2.2 nm in the case of the method **1b** based on the most intense (111) reflection. A more accurate size and size distribution of the composites was derived from transmission electron microscopy (TEM) with the images shown in Fig. 2, and in the Supp. Info. Fig. S4 and S5. Small nanoparticles with narrow size distributions were obtained after 90 min (**1a**) and 3 × 20 min (**1b**) from microwave reaction, with a medium diameter of 1.0 ±0.4 nm (**1a**)

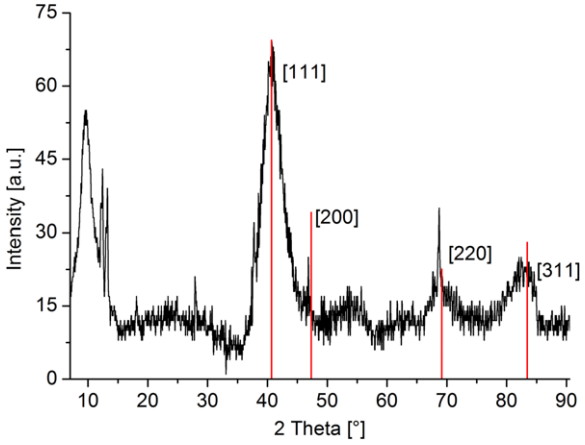

Fig. 1. Powder X-ray diffractogram of Ir@TRGO (Method **1a**) synthesized in [BMIm][BF_4]. Reference data in red for Ir metal is taken from the crystallographic open database, COD 9008470. The 2 Theta values between 5 and 25° correspond to the reflections of TRGO and in particular at 10° to residual GO (see Supp. Info. Fig. S1). (For interpretation of the references to color in this figure legend, the reader is referred to the web version of this article.)

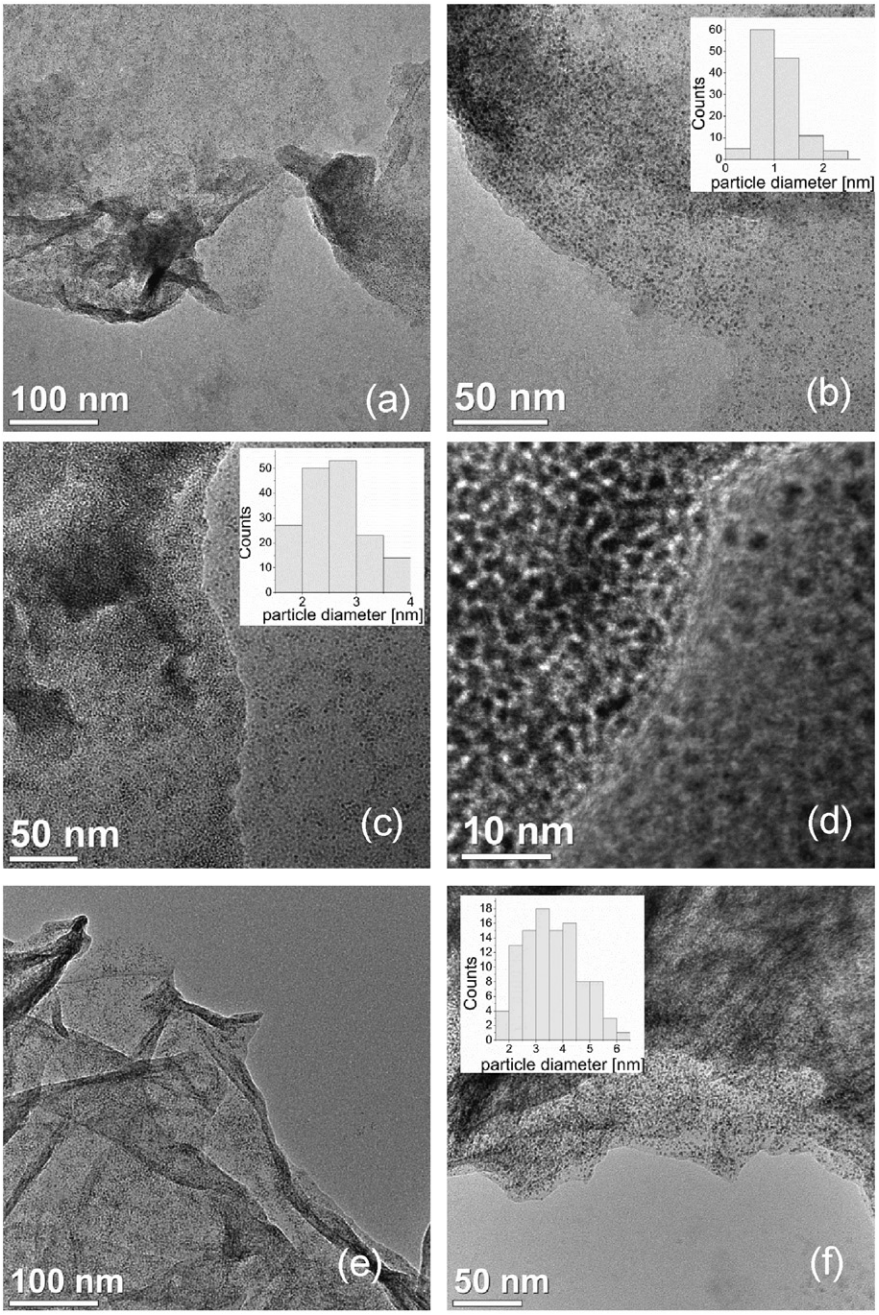

Fig. 2. TEM images of Ir@TRGO nanomaterials synthesized in [BMIm][BF_4] using microwave irradiation **1a** (a–b), **1b** (c–d) and e-beam irradiation **2** (e–f). Particle diameter distribution from 150 particles each is depicted in the inserted histograms. Additional TEM images for method **1a** and **1b** are shown in Fig. S4 and S5 in Supp. Info.

and 2.7 ±0.7 nm (**1b**), respectively (Table 1). The e-beam irradiation method (**2**) gave larger particles with a size distribution of 3.6 ±1.0 nm albeit of no crystallinity (Fig. S3).

The metal content of the Ir@TRGO composites was determined by atomic absorption spectrometry (AAS) between 3.6 and 7.2 wt%, depending on the method (Table 1). An elemental analysis by energy dispersive X-ray spectroscopy (Fig. S6 to S8 in supp. info.) only gave the expected bands for Ir metal (Ir-Lα, -Lγ, -Lλ1, -Mα, -Mγ) besides the bands for carbon and copper of the TRGO and the carbon-coated copper grid.

Infrared spectroscopy (IR) was used to follow and verify the decomposition of $Ir_4(CO)_{12}$. The IR spectra of the Ir@TRGO products in Fig. 3 still show weak absorptions for carbonyl bands at 2021 and 2058 cm^{-1}, which correspond to the CO stretching bands from the $Ir_4(CO)_{12}$ starting material. Hence, it can be concluded that either

Table 1
Ir@graphene nanomaterials synthesized in [BMIm][BF_4].

Method[a]	PXRD diameter distribution $\emptyset \pm \sigma$ (nm)[b]	TEM diameter distribution $\emptyset \pm \sigma$ (nm)[c]	Metal content (wt %)[d]
1a	1.2	1.0 ±0.4	4.9
1b	2.2	2.7 ±0.7	3.6
2	[e]	3.6 ±1.0	7.2

[a] Ir@TRGO nanomaterials were heated under microwave irradiation for 90 min (**1a**) and 3 × 20 min (**1b**) or by e-beam irradiation (**2**).
[b] From PXRD by the Scherrer equation based on the (111) reflection.
[c] Determined by TEM (cf. Fig. 2).
[d] Determined by AAS.
[e] The e-beam irradiation sample failed several times to give a PXRD.

residual $Ir_4(CO)_{12}$ precursor is still present or, more likely, that CO is bound to the surface of the iridium nanoparticles.

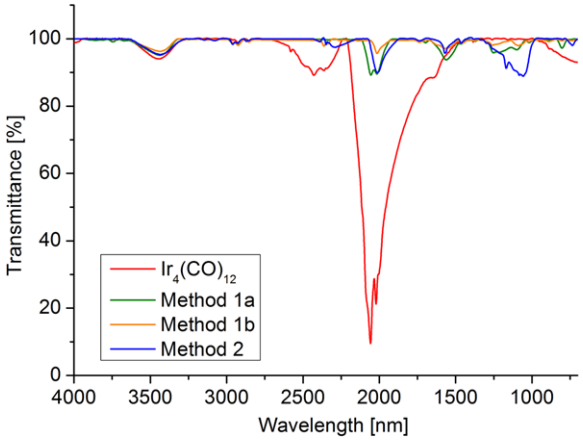

Fig. 3. Comparison of IR spectra of the Ir@TRGO composites synthesized by different methods (cf. Scheme 1) from $Ir_4(CO)_{12}$.

2.2. Hydrogenation of benzene to cyclohexane

The Ir@TRGO composite nanomaterials were tested for the industrially relevant hydrogenation of benzene to cyclohexane (Scheme 2) [60,61].

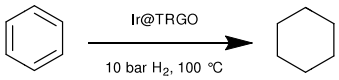

Scheme 2. Hydrogenation of benzene to cyclohexane with Ir@TRGO.

All catalytic reactions were done under inert atmosphere in a Büchi stainless-steel autoclave provided with a glass inlay to avoid any influence of the steel surface. The precursor material $Ir_4(CO)_{12}$ was also tested in 10 consecutive runs for benzene hydrogenation reaction, albeit without giving any activity.

The Ir@TRGO composite was suspended together with the benzene substrate in the autoclave. The hydrogenation reaction was carried out solvent-free at 100 °C at a constant pressure of 10 bar of H_2 with monitoring of the H_2 uptake over time (Figs. 4 and 5, Fig. S9 and S10). After one hour the reaction was stopped and cooled to room temperature. The products were condensed under vacuum in a cold trap and the composition was determined by GC. The catalyst can be recovered and re-used for at least five to ten times, without a significant loss of activity (Table 2).

For the Ir@TRGO nanocomposites synthesized by method **1b**, it could be observed that the catalyst is less active in the first runs (Table 2). The Ir@TRGO catalyst from method **1b** increased its activity to a maximum activity in about run 6 or 7 with TOF $=\sim$ 6300 or 10,300 h^{-1} depending on the experiment (Fig. S10c). The activity increase seen with Ir@TRGO **1b** may also be due to the initially still present CO coverage (cf. Fig. 3) of active sites. For Ir@TRGO synthesized by method **2** the activity was at maximum with the first run with no further increase (Fig. 5, Table 2). Catalytic tests for Ir@TRGO by method **1a** are given in the Supp. Info (Fig. S9, Tab. S1).

Conversion of benzene to cyclohexane was determined by H_2-gas uptake. Additional GC analyses also showed in all the cases cyclohexane as the only product without the presence of the cyclohexene intermediate.

In the case of the Ir@TRGO nanomaterials we found that the slightly larger nanoparticles from method **2** (3.6 ±1.0 nm diameter) gave initially a higher activity during the first and next runs (Table 2) compared to the smaller nanoparticles **1b** (2.7 ±0.7 nm diameter). The latter only increased in activity after run 4.

Table 2
Hydrogenation of benzene to cyclohexane by Ir@TRGO nanomaterials[a].

Catalyst[b]	Conversion (%)[e]		TOF (h^{-1})[f]	
$Ir_4(CO)_{12}$	None			
	–			
Ir@TRGO **1b**[c]	Exp. 1	Exp. 2	Exp. 1	Exp. 2
run 1	59.8	52.6	2210	4478
run 2	76.0	80.4	3033	7909
run 3	92.3	80.4	3325	9411
run 4[g]	87.3	40.2[g]	3358	4124
run 5[g]	69.8[g]	95.9	3668	10232
run 6	91.0	95.9	6251	9750
run 7	89.8	80.4	5104	10280
run 8	83.5	92.8	4879	9797
run 9	91.0	80.4	4678	9959
run 10	91.0	95.9	4326	10159
Ir@TRGO **2**[d]				
run 1		97.4		4861
run 2		90.8		3870
run 3		89.7		3723
run 4		96.3		4582
run 5		52.5		2194

[a] Hydrogenation reactions were done at 100 °C, 10 bars of H_2 and using a Büchi stainless-steel autoclave with a Büchi press-flow controller for measuring the H_2-uptake over the time.
[b] Molar ratio benzene/iridium, 3790 for method **1b**, experiment 1, 4490 **1b**, experiment 2 and 3943 for method **2**; see caption of Figs. 4 and 5 for further details.
[c] Synthesis by microwave irradiation; Catalytic tests for Ir@TRGO by method **1a** are given in the Supp. Info (Fig. S9).
[d] Synthesized by e-beam irradiation.
[e] Determined by H_2-uptake.
[f] TOF = mol cyclohexane × (mol Ir)$^{-1}$ × h^{-1}.
[g] Run 5 (4) in experiment 1 (2) had an instrumental error (see Fig. S10). It is important to note, however, that the problems observed in run 5 (4) were instrumental problems with the Büchi bpc gas flow controller or the autoclave. It was not a catalyst problem as the following run gave a high conversion and TOF again.

The Ir-NPs on TRGO showed a slight increase in average diameter of ∼1 nm for both samples **1b** and **2** according to TEM investigation after the 10th or 5th catalytic hydrogenation run, respectively. The Ir@TRGO **1b** synthesized by MWI (Fig. 6) exhibited a size distribution of 3.6 ±1.1 nm after ten hydrogenation runs, compared to 2.7 ±0.7 nm before. Ir@TRGO from e-beam irradiation method **2** (Fig. 7) gave a distribution of 4.6 ±1.5 nm after five hydrogenation runs, compared to 3.6 ±1.0 nm before (cf. Table 1). This leads us to conclude that there may be an optimal diameter or surface regime for the catalytic activity. Here, particles around 3.6 nm – which is the initial size from method **2** or reached during catalysis for method **1b** – can be correlated with high catalytic activity.

The size of the nanoparticles has an influence on the turnover frequency. Cunha and co-workers [62] reported for Ir nanoparticles supported on γ-Al_2O_3, that the use of smaller nanoparticles (<2 nm) gave a decreasing activity in the hydrogenation of benzene and toluene. This size dependent behavior was also observed for other catalytic reactions using supported Pt-NPs on Al_2O_3 [63] or on activated carbon [64,65], rhodium nanoparticles [66,67] or palladium nanoparticles [68].

When comparing noble-metal nanoparticle catalysts in the hydrogenation of benzene (Table 3) supported iridium nanoparticles on TRGO (TOF ∼ 10 000 h^{-1}) or zeolite [69] (TOF 3190 h^{-1}) gave a higher catalytic activity in comparison with unsupported Ir-NPs [23] in ionic liquid dispersions (∼85 h^{-1}) or in solvent-free conditions (∼71 h^{-1}) (Table 3). When considering the lower H_2 pressure of 3 bar also Ir@zeolite [69] gave high activities (Table 3).

Cyclohexene could be hydrogenated under the same mild conditions using Ir@TRGO (investigated here for the material from method **1b**). A complete conversion was achieved in less than 5 min at 100 °C and 10 bar of H_2 pressures without any loss of activity

Table 3
Hydrogenation reactions of benzene to cyclohexane by different materials.

Nanoparticle catalyst	T (°C)	p H_2 (bar)	TOF (h^{-1})	Reference
Ir@TRGO	100	10	10 000	this work
Ir@zeolite	25	3	3190	[69]
Ir-NPs	75	4	71	[23]
Ir-NP/IL	75	4	85	[23]
Ru/SiO2	100	20	5000	[70]
Rh@CNTs	25	10	2414	[72]
Rh@TRGO	50	4	310	[36]
Rh/AlO(OH)	75	4	1700	[71]
Pt-NPs	75	4	28	[73]
Pt-NP//IL	75	4	11	[73]

Table 4
Hydrogenation of cyclohexene to cyclohexane with Ir@TRGO[a] nanomaterial **1b** as catalyst[b].

Entry	Conversion (%)[c]	TON[d]	TOF (h^{-1})[e]
run 1	76.9	3070	61390
run 2	81.8	3265	65300
run 3	84.9	3390	67770
run 4	84.9	3390	67770
run 5	85.5	3410	68250

[a] Ir@TRGO method **1b**, 14 mg containing 3.6% Ir, 2.62×10^{-3} mmol Ir.
[b] Hydrogenation reactions of 0.86 g, 1.06 mL, 10.47 mmol cyclohexene were done by 100 °C, 10 bars of H_2 and 3 min, using a Büchi stainless-steel autoclave with a molar ratio of 3991 (mol cyclohexene/ mol iridium).
[c] Determined by GC analysis;.
[d] TON = mol cyclohexane/mol Ir;.
[e] TOF = mol cyclohexane × (mol Ir)$^{-1}$ × h^{-1}.

after 5 consecutive runs (Table 4). (For TEM and PXRD analysis of Ir@TRGO after 5 runs see Supp. Info.) Much higher TOFs of over 61000 h^{-1} were found in comparison with analogous Ru@TRGO (~1570 h^{-1}) and Rh@TRGO (360 h^{-1}) catalysts [36].

3. Conclusion

In summary, we report here easy and rapid methods for the synthesis of iridium@graphene nanomaterials by thermal decomposition of $Ir_4(CO)_{12}$ in the presence of a graphene material in the ionic liquid 1-butyl-3-methylimidazolium tetrafluoroborate. Decomposition energy was provided either by microwave irradiation (MWI) or by electron-beam irradiation. Both methods gave particles with average diameters of less than 5 nm without the need of additional stabilizers or capping ligands, Microwave heating resulted in slightly smaller nanoparticles.

The Ir@TRGO nanomaterials were re-usable catalysts for the relevant hydrogenation of benzene and cyclohexene. Benzene hydrogenation was successfully achieved under mild conditions (100 °C, 1 h, 10 bars) with turnover frequencies up to 10 000 h^{-1} over 5 to 10 consecutive runs with similar activities. The Ir-NPs were recovered with only slightly increased (less than 1 nm) average diameters after 5 or 10 hydrogenation runs.

A brief correlation between activity and particle size points to an optimal diameter or surface regime for the catalytic activity. Here iridium particles of 3.6 ±1.0 nm on TRGO gave the highest activity in benzene hydrogenation compared to smaller (2.7 ±0.7 nm diameter) and larger (4.6 ±1.5 nm) particles.

4. Experimental section

4.1. Materials and methods

All experiments were done using Schlenk techniques under inert atmosphere. Tetrairidium dodecacarbonyl [$Ir_4(CO)_{12}$] (98% purity) were purchased by ABCR chemicals and thermally reduced graphite oxide (TRGO) was prepared in to a two-step oxidation/thermal reduction process using natural graphite (type

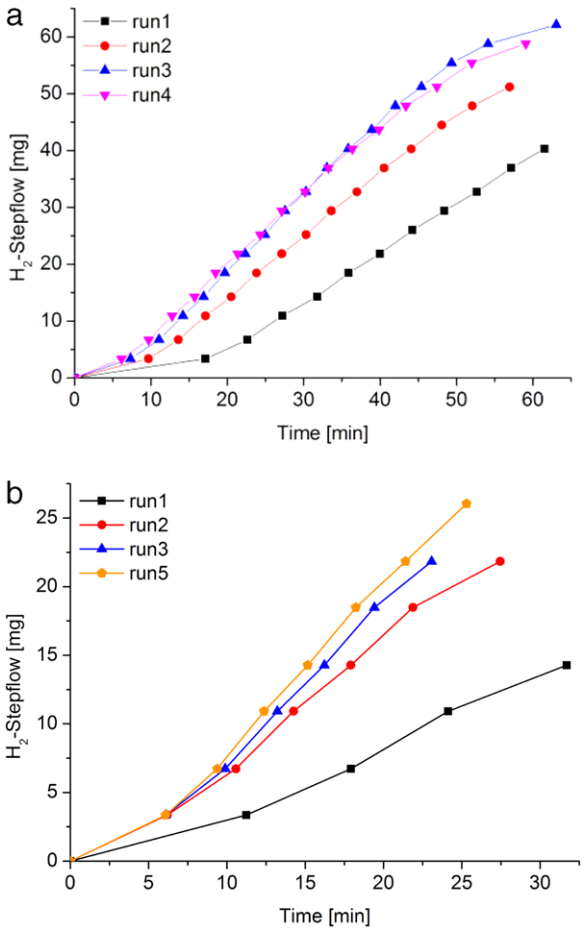

Fig. 4. H_2-uptake over time for the hydrogenation of benzene to cyclohexane with Ir@TRGO nanomaterials from method **1b** in consecutive runs with the same Ir@TRGO catalyst at 100 °C, 10 bar H_2 pressure (cf. Table 2). H_2-uptakes for the additional runs are shown in Fig. S10 in the Supporting Information. Conditions: **a** (experiment 1): benzene: 0.87 g, 1.0 mL, 11.14 mmol; Ir@TRGO catalyst: 15.7 mg, containing 3.6% Ir, 2.94×10^{-3} mmol Ir; molar benzene/metal ratio of 3790. An H_2 uptake of 67.4 mg H_2 (33.4 mmol, 802 mL) corresponds to 100% conversion. **b** (experiment 2): benzene: 0.35 g, 0.40 mL, 4.49 mmol; Ir@TRGO catalyst: 5.32 mg, containing 3.6% Ir, 1×10^{-3} mmol Ir; molar benzene/metal ratio of 4490. An H_2 uptake of 27.15 mg H_2 (13.47 mmol, 323 mL) corresponds to 100% conversion.

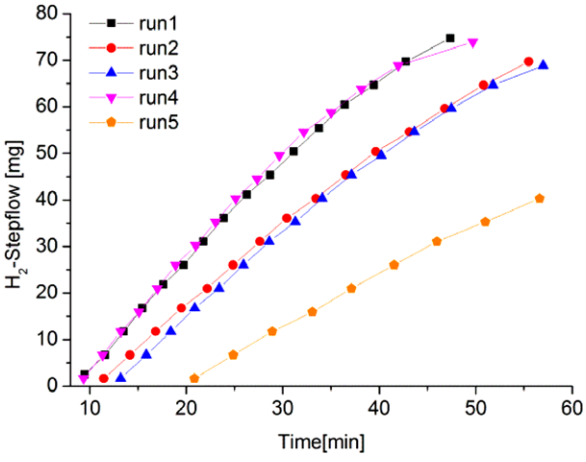

Fig. 5. H_2-uptake over time for the hydrogenation of benzene (0.99 g, 1.14 mL, 12.70 mmol) to cyclohexane with Ir@TRGO nanomaterials from method **2** in five consecutive runs with the same Ir@TRGO catalyst (8.6 mg containing 7.2% Ir, 3.22×10^{-3} mmol Ir). Molar benzene/metal ratio of 3943 at 100 °C, 10 bar H_2 pressure (cf. Table 2). An H_2 uptake of 76.8 mg (38.1 mmol, 914 mL) corresponds to 100% conversion.

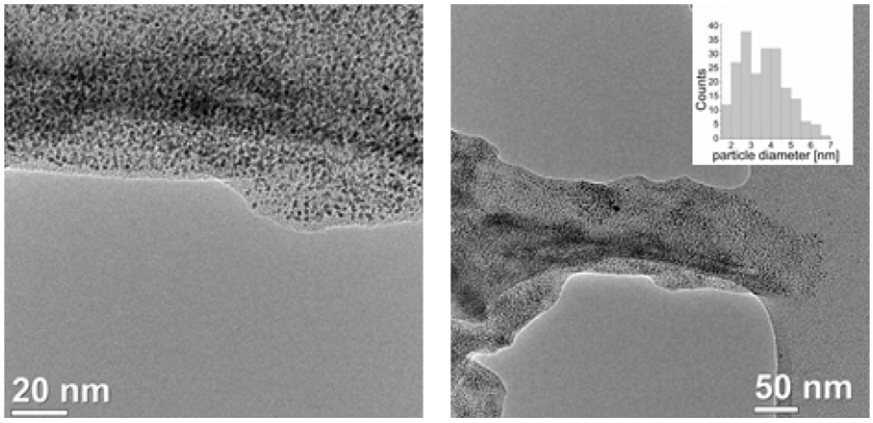

Fig. 6. TEM images of Ir@TRGO **1b** after 10 hydrogenation runs.

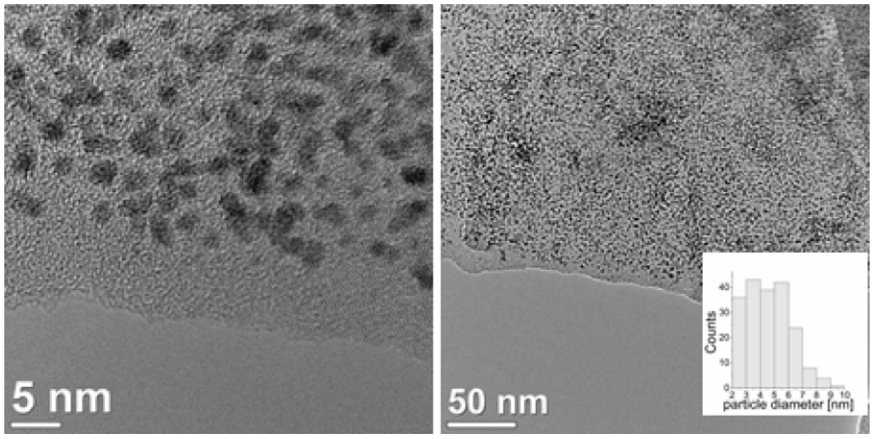

Fig. 7. TEM images of Ir@TRGO **2** after 5 hydrogenation runs.

KFL 99.5 from Kropfmühl AG, Passau, Germany) as raw material. Graphite was oxidized to graphite oxide (GO) according to the procedure described by Hummers and Offeman [74]. This oxidation incorporates functional groups like epoxy and alcohol moieties into the graphite structure. When GO is subjected to rapid heating above 400 °C the functional groups decompose into CO and CO_2 gas which exfoliates the layered GO structure into functionalized graphene sheets [75]. This thermal reduction of graphite oxide lends its name to the product (TRGO). By adjusting the reduction temperature, the degree of functionalization can be controlled. At a lower reduction temperature, more oxygen atoms remain on the TRGO surface and thereby increase the degree of functionalization. This degree of functionalization influences on the dispersibility of TRGO in polar solvents [76] and its use as a support material for metal nanoparticles. A higher degree of functionalization improves the dispersibility, e.g., in water or acetone. Therefore, it can be expected that a TRGO-material with a high degree of functionalization has a good interaction with metal particles. For these reasons we reduced GO at 400 °C and achieved an oxygen content of 21 wt% as calculated by the difference to 100e% from elemental analysis (77.9% C, 0.7% H). The benzene (VWR p.A.), and cyclohexene (Sigma Aldrich, p.A) were dried with sodium, distilled and store on 4 Å molecular sieves.

The ionic liquid, [BMIm][BF_4], was synthesized by reacting 1-methylimidazole with 1-chlorobutane to yield first [BMIm]Cl which was further reacted with HBF_4 to give [BMIm][BF_4]. The IL was dried under high vacuum (10–7 mbar) at 80 °C for several days. Quantitative anion exchange and, thus, IL purity was assessed by ion chromatography (ICS-1100, with Ion-Pac® AS22, 4 × 250 mm column) to be >99%. The water content determined by coulometric Karl Fischer titration (ECH/ANALYTIKJENA AQUA 40.00) was less than 10 ppm.

Powder X-ray diffraction patterns data were measured at on a Bruker D2 Phaser using a flat low background sample holder and Cu-Kα radiation (λ = 1.54182 Å, 35 kV) covering 2 theta angles 5–90° over a time of 8 h, that is 0.003°/s. All measurements were done at room temperature. The samples had been precipitated and washed with water and were dried under vacuum.

IR was measured on a Bruker TENSOR 37 IR spectrometer in a range from 4000 to 500 cm^{-1} in form of KBr disks.

Metal analyses were performed by flame atomic absorption spectroscopy (AAS) on a Vario 6 from Analytik Jena. Samples were digested in *aqua regia* three times, filtered and *aqua regia* was added to a final volume of 25 mL.

Transmission electron microscopy (TEM) micrographs were taken on a FEI Tecnai G20 TEM operating at an accelerating voltage of 200 kV. Samples were deposited on 200 μm carbon-coated copper grids (3.025 mm copper-grids with a 200 mesh and coated with 10 nm carbon film) from PLANO GmbH. The size distribution was determined using Gatan Digital Micrograph for 150 nanoparticles. Energy dispersive X-ray spectra were taken on a FEI Tecnai f20, detector voltage 136 kV; the exposure time for individual EDX spectra was 3 min.

Conversion of benzene to cyclohexane was determined by gas chromatography (GC) (Perkin Elmer 8500 HSB 6, equipped with a DB-5 film capillary column, 60 m × 0.32 mm, film thickness 25 μm, oven temperature 40 °C, N_2 carrier flow 120 L/min and a flame ionization detector (FID), 250 °C detector temperature). The samples were analyzed by putting a drop of the product into a GC sample vial together with 1 mL of distilled water. Also the

conversion was determined by NMR on a Bruker Avance DRX 200 (^{1}H — NMR, 200 MHz) in $CDCl_3$. Conversion of cyclohexene to cyclohexane was determined by gas chromatography (SHIMADZU, GC-2014).

4.2. Synthesis of Ir@TRGO nanoparticles in [BMIm][BF_4].

Microwave irradiation: In a typical experiment [$Ir_4(CO)_{12}$] (35.8 mg, 0.032 mmol) and TRGO (4.8 mg, 0.2 wt% related to 2.42 g [BMIm][BF_4]) were dispersed in 1-butyl-3-methylimidazolium tetrafluoroborate ([BMIm][BF_4]) (2 mL, 1.21 g/mL), sonicated at 30 ° C for 6 h and stirred at room temperature for the next 12 h.

Decomposition of the sample was done using microwave irradiation by 250 °C (200 W, 4 bars) for 90 min (Method **1a**) or 3x 20 min (Method **1b**). After heating the volatiles (CO) were removed *in vacuo*. Finally the sample was washed and centrifuged (6000 rpm × 15 min) with distilled water and dried under vacuum at 100 °C for several hours.

e-beam accelerator (Method **2**): Sample preparation and isolation were done with the same procedure as by the microwave method. The sample was decomposed by β-irradiation in a 10 MeV IBA Rhodotron e-beam accelerator as follows: energy of the electron 10 MeV; energy uptake up to 90 kGy, each run 30 kGy; radiation 30–58 kGy/s, time 3 × 1 s (Herotron E-Beam Service GmbH)[d].

4.3. Hydrogenation reactions

All catalytic processes were done using stainless-steel autoclaves under inert atmosphere. Each autoclave was equipped with a glass inlay to avoid any effect of the steel in the reaction.

The desired amount of catalyst (*Benzene*: Ir@TRGO **1b**, 15.71 mg containing 3.6% Ir, 2.94 × 10^{-3} mmol Ir; Ir@TRGO **2,** 8.6 mg containing 7.17% Ir, 3.22 × 10^{-3} mmol Ir or *cyclohexene*: Ir@TRGO **1b** 14 mg containing 3.6% Ir, 2.62 × 10^{-3} mmol Ir) and the substrate (for **1b**: benzene 0.87 g, 1.0 mL, 11.14 mmol or cyclohexene: 0.86 g, 1.06 mL, 10.47 mmol and for **2**: benzene 0.99 g, 1.14 mL, 12.70 mmol) were loaded in the autoclave under inert atmosphere. The autoclave was purged three times with H_2 and then charge with 10 bars of H_2. The stirring rate was 800 rpm and the heating temperature 100 °C. After one hour (benzene) or 3 min (cyclohexene) the process was stopped and cooled down. The organic volatile products were condensed under vacuum and condensed in a cool trap and analyzed by GC. Conversion of benzene was determined by H_2 uptake.

Re-use and recycling of the catalyst: Once the product was removed under vacuum, the autoclave was charged again with the desired amount of benzene and close properly for the next run.

All syntheses and catalytic runs were repeated at least twice to ensure reproducibility (see Fig. 4, Table 2).

Acknowledgments

Authors are thankful to the Deutsche Forschungsgemeinschaft (DFG) for grant Ja466/31-1 within SPP 1708, Herotron E-Beam Service GmbH, Bitterfeld-Wolfen for β-irradiation decomposition and to Dr. Juri Barthel and the Ernst Ruska-Centre (ER-C) for Microscopy and Spectroscopy with Electrons, Jülich Research Centre and RWTH Aachen University, 52425 Jülich (Germany) for help and access to the HR-TEM facilities. We thank Mrs. Christina Rutz for the IL-anion analysis.

Appendix A. Supplementary data

Supplementary material (additional PXRD patterns, TEM images, EDX spectra and information to catalytic hydrogenation runs of **1a** and **1b**) related to this article can be found online at http://dx.doi.org/10.1016/j.nanoso.2015.07.001.

References

[1] K. Saha, S.S. Agasti, C. Kim, X. Li, V.M. Rotello, Chem. Rev. 112 (2012) 2739–2779.
[2] H. Goesmann, C. Feldmann, Angew. Chem. Int. Ed. 49 (2010) 1362–1395.
[3] J.A. Dahl, B.L.S. Maddux, J.E. Hutchison, Chem. Rev. 107 (2007) 2228–2269.
[4] D. Astruc, Nanoparticles and Catalysis, Wiley-VCH, Weinheim, 2007.
[5] J.D. Scholten, B.C. Leal, J. Dupont, ACS Catal. 2 (2012) 184–200.
[6] D. Astruc, F. Lu, J.R. Aranzaes, Angew. Chem. Int. Ed. 44 (2005) 7852–7872.
[7] C. Pan, K. Pelzer, K. Philippot, B. Chaudret, F. Dassenoy, P. Lecante, M.J. Casanove, J. Am. Chem. Soc. 123 (2001) 7584–7593.
[8] J.D. Aiken III, R.G. Finke, J. Am. Chem. Soc. 121 (1999) 8803–8810.
[9] T. Welton, Chem. Rev. 99 (1999) 2071–2084.
[10] C. Feldmann, Introduction to special issue on ionic liquids in chemical synthesis, Z. Naturforsch. 68b (2013) 1057.
[11] C. Janiak, Z. Naturforsch. 68b (2013) 1059–1089.
[12] C. Janiak, Metal nanoparticle synthesis in ionic liquids, in: J. Dupont, L. Kollar (Eds.), Ionic Liquids (ILs) in Organometallic Catalysis, in: Topics in Organometallic Chemistry, vol. 51, Springer, Heidelberg, 2015, pp. 17–53.
[13] C. Janiak, Metal nanoparticle synthesis in ionic liquids, in: C. Hardacre, V. Parvulescu (Eds.), Catalysis in Ionic Liquids: From Catalyst Synthesis to Application, RSC Publishing, Cambridge, 2014, pp. 537–577 (chapter 11).
[14] J. Dupont, J.D. Scholten, Chem. Soc. Rev. 39 (2010) 1780–1804.
[15] P. Wasserscheid, W. Keim, Angew. Chem. Int. Ed. 39 (2000) 3773–3789.
[16] L. Taubert, Z. Li, Dalton Trans. (2007) 723–727.
[17] E. Redel, J. Krämer, R. Thomann, C. Janiak, J. Organomet. Chem. 694 (2009) 1069–1075.
[18] C. Vollmer, E. Redel, K. Abu-Shandi, R. Thomann, H. Manyar, H. Hardacre, Chem. Eur. J. 16 (2010) 3849–3858.
[19] K. Schütte, H. Meyer, C. Gemel, J. Barthel, R.A. Fischer, C. Janiak, Nanoscale 6 (2014) 3116–3126.
[20] K. Klauke, B. Hahn, K. Schütte, J. Barthel, C. Janiak, Nano-Struct. Nano-Objects 1 (2015) 24–31.
[21] G.S. Fonseca, G. Machado, S.R. Teixeira, G.H. Fecher, J. Morais, M.C.M. Alves, J. Dupont, J. Colloid Interface Sci. 301 (2006) 193–204.
[22] G.S. Fonseca, J.B. Domingos, F. Nome, J. Dupont, J. Mol. Catal. A 248 (2006) 10–16.
[23] G.S. Fonseca, A.P. Umpierre, P.F.P. Fichtner, S.R. Teixeira, J. Dupont, Chem. Eur. J. 9 (2003) 3263–3269.
[24] J. Dupont, G.S. Fonseca, A.P. Umpierre, P.F.P. Fichter, S.R. Teixeira, J. Am. Chem. Soc. 124 (2002) 4228–4229.
[25] E. Redel, M. Walter, R. Thomann, L. Hussein, M. Krüger, C. Janiak, Chem. Commun. 46 (2010) 1159–1161.
[26] E. Redel, M. Walter, R. Thomann, C. Vollmer, L. Hussein, H. Scherer, M. Krüger, C. Janiak, Chem. Eur. J. 15 (2009) 10047–10059.
[27] E. Redel, R. Thomann, C. Janiak, Inorg. Chem. 47 (2008) 14–16.
[28] P. Migowski, G. Machado, S.R. Teixeira, M.C.M. Alves, J. Morais, A. Traverse, J. Dupont, Phys. Chem. Chem. Phys. 9 (2007) 4814–4821.
[29] T. Gutel, C.C. Santini, K. Philippot, A. Padua, K. Pelzer, B. Chaudret, Y. Chauvin, J.-M. Basset, J. Mater. Chem. 19 (2009) 3624–3631.
[30] T. Gutel, J. Garcia-Anton, K. Pelzer, K. Philippot, C.C. Santini, Y. Chauvin, B. Chaudret, J.-M. Basset, J. Mater. Chem. 17 (2007) 3290–3292.
[31] G. Salas, A. Podgorsek, P.S. Campbell, C.C. Santini, A.A.H. Pádua, M.F. Costa Gomes, K. Philippot, B. Chaudret, M. Turmine, Phys. Chem. Chem. Phys. 13 (2011) 13527–13536.
[32] E.T. Silveira, A.P. Umpierre, L.M. Rossi, G. Machado, J. Morais, G.V. Soares, I.J.R. Baumvol, S.R. Teixeira, R.F.P. Fichtner, J. Dupont, Chem. Eur. J. 10 (2004) 3734–3740.
[33] D. Marquardt, J. Barthel, M. Braun, C. Ganter, C. Janiak, Cryst. Eng. Comm. 14 (2012) 7607–7615.
[34] C. Vollmer, C. Janiak, Coord. Chem. Rev. 255 (2011) 2039–2057.
[35] C. Vollmer, M. Schröder, Y. Thomann, R. Thomann, C. Janiak, Appl. Catal. A 425-426 (2012) 178–183.
[36] (a) D. Marquardt, C. Vollmer, R. Thomann, P. Steurer, R. Mülhaupt, E. Redel, C. Janiak, Carbon 49 (2011) 1326–1332;
(b) R. Marcos Esteban, K. Schütte, D. Marquardt, J. Barthel, F. Beckert, R. Mülhaupt, C. Janiak, Nano-Struct. Nano-Objects 1 (2015) http://dx.doi.org/10.1016/j.nanoso.2015.07.002.
[37] D. Marquardt, Z. Xie, A. Taubert, R. Thomann, C. Janiak, Dalton Trans. 40 (2011) 8290–8293.
[38] J. Krämer, E. Redel, R. Thomann, C. Janiak, Organometallics 27 (2008) 1976–1978.
[39] E. Redel, R. Thomann, C. Janiak, Chem. Commun. (2008) 1789–1791.
[40] J.M. Zhu, Y.H. Shen, A.J. Xie, L.G. Qiu, Q. Zhang, X.Y. Zhang, J. Phys. Chem. C. 111 (2007) 7629–7633.
[41] M.A. Firestone, M.L. Dietz, S. Seifert, S. Trasobares, D.J. Miller, N.J. Zaluzec, Small 1 (2005) 754–760.
[42] F. Endres, D. MacFarlane, A. Abbott, Electrodeposition from Ionic Liquids, Wiley-VCH, Weinheim, 2008.
[43] D. Marquardt, C. Janiak, Nachr. Chemie 61 (2013) 754–757.
[44] R. Venkatesan, M.H.G. Prechtl, J.D. Scholten, R.P. Pezzi, G. Machado, J. Dupont, J. Mater. Chem. 21 (2011) 3030- 3036–3030- 3036.
[45] K. Schütte, A. Doddi, C. Kroll, H. Meyer, C. Wiktor, C. Gemel, G. van Tendeloo, R.A. Fischer, C. Janiak, Nanoscale 6 (2014) 5532–5544.
[46] S. Schauermann, N. Nilius, S. Shaikhu, H.-J. Freund, Acc. Chem. Res. 46 (2013) 1673–1681.
[47] P.D. Kent, J.E. Mondloch, R.G. Finke, J. Am. Chem. Soc. 136 (2014) 1930–1941.
[48] H. Park, Mater. Chem. Phys. 133 (2012) 1050–1054.

[49] H. Park, J.S. Kim, B.G. Choi, S.M. Jo, D.Y. Kim, W.H. Hong, S.-Y. Jang, Carbon 48 (2010) 1325–1330.
[50] Y. Gao, S. Li, B. Zhao, Q. Zhai, A. Lita, N.S. Dalal, H.W. Kroto, S.F.A. Acquah, Carbon 77 (2014) 705–709.
[51] C.N.R. Rao, A.K. Sood, K.S. Subrahmanyam, A. Govindaraj, Angew. Chem. Int. Ed. 48 (2009) 7752–7777.
[52] Z. Wang, K. Shang, J. Dong, Z. Cheng, S. Ai, Microchim. Acta 179 (2012) 227–234.
[53] X.-Y. Yan, X.-L. Tong, Y.-F. Zhang, X.-D. Han, Y.-Y. Wang, G.-Q. Jin, Y. Qina, X.-Y. Guo, Chem. Commun. 48 (2012) 1892–1894.
[54] D. Marquardt, F. Beckert, F. Pennetreau, F. Tölle, R. Mülhaupt, O. Riant, S. Hermans, J. Barthel, C. Janiak, Carbon 66 (2014) 285–294.
[55] K. Gotoh, K. Kawabata, E. Fujii, K. Morishige, T. Kinumoto, Y. Miyazaki, H. Ishida, Carbon 47 (2009) 2112–2142.
[56] M.C. Rath, D.B. Naik, S.K. Sarkar, J. Nucl. Mater. 438 (2013) 26–31.
[57] S. Singh, M.C. Rath, A.K. Singh, S.K. Sarkar, T. Mukherjee, Mater. Chem. Phys. 124 (2010) 6–9.
[58] S. Singh, M.C. Rath, A.K. Singh, T. Mukherjee, O.D. Jayakumar, A.K. Tyagi, S.K. Sarkar, Radiat. Phys. Chem. 80 (2011) 736–741.
[59] S. Seino, T. Kinoshita, E.T. Nakagawa, T. Kojima, R. Taniguci, S. Okuda, T.A. Yamamoto, J. Nanopart. Res. 10 (2008) 1071–1076.
[60] A. Stanislaus, B.H. Cooper, Catal. Rev. 36 (1994) 75–123.
[61] R.C. Larock, Comprehensive Organic Transformations, Wiley-VCH, New-York, 1999.
[62] D.S. Cunha, G.M. Cruz, Appl. Catal. A: General 236 (2002) 55–66.
[63] H. Shi, O.Y. Gutiérrez, H. Yang, N.D. Browning, G.L. Haller, J.A. Lercher, ACS Catal. 3 (2013) 328–338.
[64] B. Meryemoglu, S. Irmak, A. Hasanoglu, O. Erbatur, B. Kaya, Fuel 134 (2014) 354–357.
[65] T. Frelink, W. Visscher, J.A.R. van Veen, J. Electroanalyt. Chem. 382 (1995) 65–72.
[66] Y. Zhang, D.A.J.M. Ligthart, X.-Y. Quek, L. Gao, E.J.M. Hensen, Int. J. Hydrog. Energy 39 (2014) 11537–11546.
[67] E. Galicia, G. Diaz, S. Fuentes, Catalysis 38 (1987) 11–19.
[68] O.M. Wilson, M.R. Knecht, J.C. Garcia-Martinez, R.M. Crooks, J. Am. Chem. Soc. 128 (2006) 4510–4511.
[69] Y. Tonbul, M. Zahmakiran, S. Ozkar, Appl. Catal. B: Environmental. 148-149 (2014) 466–472.
[70] X. Kang, J. Zhang, W. Shang, T. Wu, P. Zhang, B. Han, Z. Wu, G. Mo, X. Xing, J. Am. Chem. Soc. 136 (2014) 3768–3771.
[71] I.-S. Park, M.S. Kwon, K.Y. Kang, J.S. Lee, J. Parka, Adv. Synth. Catal. 349 (2007) 2039–2047.
[72] H.-B. Pan, C.M. Wai, J. Phys. Chem. C 113 (2009) 19782–19788.
[73] C.W. Scheeren, G. Machado, J. Dupont, P.F.P. Fichtner, S.R. Texeira, Inorg. Chem. 42 (2003) 4738–4742.
[74] W.S. Hummers, R.E. Offeman, J. Am. Chem. Soc. 80 (1958) 1339.
[75] D.R. Dreyer, S. Park, C.W. Bielawski, R.S. Ruoff, Chem. Soc. Rev. 39 (2010) 228–240.
[76] F.J. Tölle, M. Fabritius, R. Mülhaupt, Adv. Funct. Mater. 22 (2012) 1136–1144.